Society For Biomaterials

Drug release and bone growth studies of antimicrobial peptide-loaded calcium phosphate coating on titanium

Mehdi Kazemzadeh-Narbat,[1] Shahryar Noordin,[2] Bassam A. Masri,[2] Donald S. Garbuz,[2] Clive P. Duncan,[2] Robert E. W. Hancock,[3] Rizhi Wang[1]

[1]Department of Materials Engineering, University of British Columbia, Vancouver, British Columbia, Canada
[2]Department of Orthopaedics, University of British Columbia, Vancouver, British Columbia, Canada
[3]Department of Microbiology and Immunology, University of British Columbia, Vancouver, British Columbia, Canada

Received 5 September 2011; revised 30 January 2012; accepted 2 February 2012
Published online 00 Month 2012 in Wiley Online Library (wileyonlinelibrary.com). DOI: 10.1002/jbm.b.32701

Abstract: Preventing infection is one of the major challenges in total hip and joint arthroplasty. The main concerns of local drug delivery as a solution have been the evolution of antibiotic-resistant bacteria and the potential inhibition of osseointegration caused by the delivery systems. This work investigated the *in vitro* drug release, antimicrobial performance, and cytotoxicity, as well as the *in vivo* bone growth of an antimicrobial peptide loaded into calcium phosphate coated Ti implants in a rabbit model. Two potent AMP candidates (HHC36: KRWWKWWRR, Tet213: KRWWKWWRRC) were first investigated through an *in vitro* cytotoxicity assay. MTT absorbance values revealed that HHC36 showed much lower cytotoxicity (minimal cytotoxic concentration 200 μg/mL) than Tet 213 (50 μg/mL). The AMP HHC36 loaded onto CaP (34.7 ± 4.2 μg/cm^2) had a burst release during the first few hours followed by a slow and steady release for 7 days as measured spectrophotometrically. The CaP-AMP coatings were antimicrobial against *Staphylococcus aureus* and *Pseudomonas aeruginosa* strains in colony-forming units (CFU) *in vitro* assays. No cytotoxicity was observed on CaP-AMP samples against MG-63 osteoblast-like cells after 5 days *in vitro*. In a trabecular bone growth *in vivo* study using cylindrical implants, loading of AMP HHC36 did not impair bone growth onto the implants. Significant bone on-growth was observed on CaP-coated Ti with or without HHC36 loading, as compared with Ti alone. The current AMP-CaP coating thus offers *in vivo* osteoconductivity to orthopedic implants. It also offers *in vitro* antimicrobial property, with its *in vivo* performance to be confirmed in future animal infection models. © 2012 Wiley Periodicals, Inc. J Biomed Mater Res Part B: Appl Biomater 00B:000–000, 2012.

Key Words: peri-implant infection, calcium phosphate coating, antimicrobial peptide, bone growth, titanium, orthopedic implants

How to cite this article: Kazemzadeh-Narbat M, Noordin S, Masri BA, Garbuz DS, Duncan CP, Hancock Robert E. W., Wang R. 2012. Drug release and bone growth studies of antimicrobial peptide-loaded calcium phosphate coating on titanium. J Biomed Mater Res Part B 2012:00B:000–000.

INTRODUCTION

The demand for artificial joints is constantly rising due to the increasing age of our populations with increasing prevalence of osteoarthritis, failure of previously implanted components and the steady increase of trauma patients requiring joint replacement surgery.[1,2] Implant-associated infection as the major cause of implant revision has been a serious challenge to joint arthroplasty.[3–5] Early stage infection occurs after implantation when the host local defense system is impaired due to surgical trauma. At this critical time, highly virulent bacteria, such as Gram-positive *Staphylococcus aureus (S. aureus)*, and opportunistic pathogens like Gram-negative *Pseudomonas aeruginosa (P. aeruginosa)* are colonized on the implant surface.[6–8] The further development of a biofilm results in resistance to antibiotic prophylaxis. Conventional systemic administration of antibiotics without implant removal has difficulty eradicating this infection, and radical debridement surgery including implant exchange/retention in addition to prolonged and high dose antibiotic therapy is usually required.[1,9–13]

Antibacterial coatings have attracted wide attention as a technique of preventing implant-associated infections at the site of implant. Antibacterial coatings include adhesion-resistant coatings and coatings releasing antimicrobial agents.[10,14,15] One challenge facing the antibacterial coatings is to inhibit bacteria growth onto the implant surface without impairing osseointegration. The other challenge is to develop novel classes of broad-spectrum antimicrobial agents that do not induce development of multi drug-resistant (MDR) strains, which has been a serious concern for most traditional antibiotics. After more than two decades of research and development, antimicrobial peptides (AMP) are now well recognized as promising novel agents against MDR pathogens.[16–18] Existing in all forms of life,

Correspondence to: R. Wang; e-mail: rzwang@mail.ubc.ca
Contract grant sponsors: Natural Sciences and Engineering Research Council of Canada; the Canadian Institutes of Health Research

natural AMPs are relatively short (12 to 50 amino acids), cationic (+2 to +9), and amphiphilic (>50% hydrophobic amino acids).[19–21] They often have broad-spectrum bactericidal activity against both Gram-negative and Gram-positive bacteria. The complexity of their antimicrobial mechanisms makes it extremely difficult for AMP resistant mutant selection.[17,20,22] In addition, cationic AMPs kill bacteria more rapidly than conventional antibiotics and can often promote favorable host innate immunity without causing unfavorable immunotoxicities or immunogenicity.[23] Despite of the promising potency of AMPs, there are still issues that need to be solved before clinical applications including tissue and cell interactions and potential cytotoxicities associated with high concentrations of soluble AMPs.[23,24]

In a previous report, we proposed to deliver AMPs through a layer of calcium phosphate (CaP) coating on titanium surface.[10] The idea was to combine the antimicrobial activity of AMPs with the potential osteoconductivity of the CaP coating. Although antimicrobial activity was demonstrated, the osteoconductivity of the drug-loaded coating has yet to be verified in an animal model. The AMP used earlier had a cysteine introduced at one end of the peptide to enable surface conjugation.[25] It was not clear whether the cysteine residue, when present in unconjugated form, would cause any negative effect on biocompatibility.

In this study, we first compared two antimicrobial peptides, HHC36 (KRWWKWWRR) and its cysteinylated form Tet213, in terms of their *in vitro* biocompatibility, cytotoxicity, and bactericidal activity. In the second stage, we studied the effect of AMP on bone growth in a rabbit model using CaP coated-Ti implants.

MATERIALS AND METHODS

Implants and CaP coating deposition

Commercially pure titanium plates (Goodfellow, USA) of dimensions 10 × 10 × 0.5 mm^3 were prepared for *in vitro* tests. All Ti specimens were ground by a 320 grit sandpaper followed by thorough cleaning with alkaline detergent (Fisher Scientific SF105), ultrasonically washing with acetone, 70% ethanol, and distilled water for 10 min, respectively, to remove any residuals, and grease. The cleaned samples were then chemically etched by 2% hydrofluoric acid (Fisher Scientific) for 1 min and ultrasonically washed in distilled water followed by air-drying at room temperature. The calcium phosphate coating applied onto Ti surfaces was applied using our previously reported electrolyte deposition (ELD) technique.[10,26,27] Briefly, a two-electrode base ELD (Ti as cathode and platinum as anode) with electrode working distance of 3 cm was employed for CaP deposition. The electrolyte composed of 5.25 m*M* of $Ca(NO_3)_2$ (Sigma Aldrich), 10.5 m*M* of $NH_4H_2PO_4$ (Fisher Scientific), and 150 m*M* of NaCl (Fisher Scientific). After increasing the pH of electrolyte to 5.30 ± 0.05 by adding drop wise NaOH (Fisher Scientific) solution, a DC voltage of 2.5 V was conducted between the electrodes for 3 h at room temperature. Based on our previous study the CaP coating thus processed was a uniform micro-porous plate-like CaP with increased pore and crystal sizes from the bottom to the surface. The coating consisted of octacalcium phosphate (OCP) with a thickness of about 7 μm, and adhered to the Ti substrate without cracks.[10]

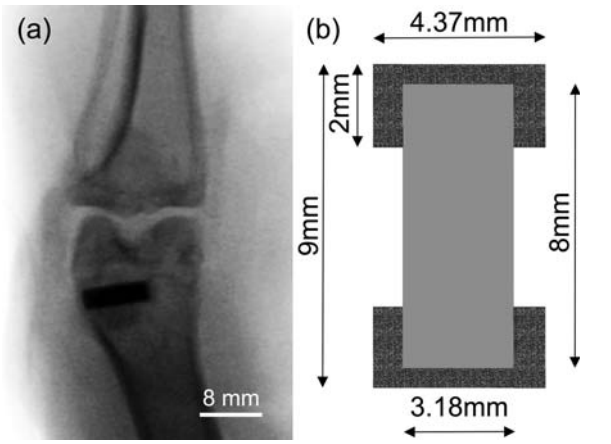

FIGURE 1. (a) X-ray image of implant position on lateral aspect of the distal portion of the rabbit femur. (b) A schematic diagram of gap model designed for bone growth study. The Ti rod is capped by PMMA bone cement creating a 0.6 mm gap distance between the Ti implant and the host bone.

For the *in vivo* bone growth study, commercially pure titanium rods (Goodfellow, USA) were machined into cylindrical implants, each 3.18 mm in diameter and 8 mm long. Three groups of cylindrical implants were used in the animal experiment, etched Ti, CaP-coated Ti (CaP), and CaP-coated Ti loaded with AMP (CaP-AMP). To investigate bone growth, a gap model was designed by capping both ends of implant cylinders with polymethylmethacrylate (PMMA) bone cement. Each cap had an outer diameter of 4.37 mm, height of 2 mm, which made the total length of implant including caps 9 mm. This model provided a gap space of 0.6 mm and a gap volume of 35.3 mm^3 [Figure 1(b)].[27] The introduction of a gap was based on our previous animal model.[27] The idea was to simulate a real situation in implant surgery. Such a model also made it easier to characterize new bone growth. F1

AMP loading on CaP

On the basis of the most recent quantitative structure-activity relationships (QSAR) analysis, short cationic AMPs with high antimicrobial activity, namely HHC36 (KRWWKWWRR) and its cysteinylated derivative Tet213 (KRWWKWWRRC), were screened.[28,29] To select the best AMP for bone growth investigation, antimicrobial testing, and the MTT cytotoxicity assay using MG-63 osteoblast-like were performed.

To load the HHC36 into CaP coating, a peptide solution with a concentration of 1 mg/mL was prepared by dissolving 1 mg of HHC36 in 1 mL of simple phosphate solution containing 50 m*M* of NaH_2PO_4 (Calbiochem) in distilled water. The buffer pH was adjusted to 7.5 by adding 0.1*M* NaOH prior to addition of AMP. The CaP-coated Ti specimens were immersed into peptide solution separately for 1 h and slowly shaken at room temperature. To remove the residual peptide samples were then washed three times for

1 min with phosphate buffer. The implants were then gently air-dried and stored in safe dry containers.

AMP detection and release experiment

The total AMP concentration loaded on CaP was measured by UV/Vis spectroscopy by recording the absorption peak at 280 nm, which is the characteristic excitation wavelength for tryptophan.[30,31] The AMP was removed from the CaP coating by ultrasonically dissolving six independent AMP-CaP plate samples with HCl (0.1*N*) at room temperature for 30 min. A series of standards in the concentration range 2–100 μg/mL of HHC36 in 0.1*N* HCl were prepared in triplicate to calibrate the system. AMP quantification was then calculated based on the external standard method.

To determine the release profile of AMP from the CaP coating, three CaP-AMP specimens were immersed in 1 mL of PBS (pH 7.4) in a glass vial while gently rotating at 37°C. After 30 min, 90 min, 150 min, 270 min, 1 day, 3 day, and 7 day, 500 μL of PBS was sampled and fresh PBS was replenished to each sample. Each release test was done in triplicate. The samples were stored at −20°C and the AMP cumulative release ratio was calculated by using UV/Vis spectroscopy.

Antimicrobial activity

The antimicrobial effect of CaP-AMP was tested by a survival assay by counting the residual number of colony-forming units (CFU) in triplicate experiments. The specimens were evaluated against *S. aureus* (ATCC 25293) as well as *P. aeruginosa* (H1001:*lux*CDABE) strains. The bacteria strains were grown in Mueller-Hinton agar (MHA; Difco) and subcultured overnight at 37°C incubator under aerobic conditions. After the appearance of colonies, two colonies were harvested from the MHA agar and suspended in Mueller Hinton Broth (MHB; Difco) overnight while shaking in the incubator. The bacteria status in the mid logarithmic phase of grow was determined by suspending 100 μL of each bacteria solution into 5 mL of MHB following incubation at 37°C for 1 h. *P. aeruginosa*, and *S. aureus* bacterial suspensions were diluted by MHB, and adjusted to the final concentration of 10^{-6} CFU/mL using spectrophotometer. Six CaP-AMP specimens ($10 \times 10 \times 0.5$ mm^3) were rinsed with phosphate buffer saline (PBS) three times, then 400 μL of each bacterial suspension was pipette onto two different groups of samples. The bacterial suspension alone was considered as a negative control group. After incubating the samples for 30, 90, 150, and 270 min, the residual bacteria in 10 μL were spotted on nutrient MHA agar. Corresponding agar plates were incubated at 37°C overnight, and bacterial survival was evaluated by CFU measurement.

Cell viability

The viability of MG-63 osteoblast-like cells derived from human osteosarcoma (ATCC CRL-1427, USA) was studied by measuring the mitochondrial dehydrogenase activity using a modified MTT (3-(4,5-dimetyl-2-tiazolyl)-2,5-diphenyl-2H-tetrazolium bromide) (Biotium) reduction assay. The cells were cultured in a medium consisting of Dulbecco's Modified Eagle Medium (DMEM, GIBCO), including a minimal essential medium, 10% fetal bovine serum (FBS), and 1% nonessential amino acids (GIBCO). The culture medium was refreshed at 2-day interval and the incubator ambience was maintained at 37°C under 95% humidified atmosphere with 5% CO_2. To evaluate the cytotoxicity level of HHC36 and Tet213, 10^4 cells per sample were cultured with both AMPs. Cells were incubated with different concentrations of AMPs/medium at 37°C and humidified 5% CO_2 in triplicate. Negative controls were assigned to cells cultured in fresh medium and normal conditions with no AMP. After 16 h, 100 μL MTT was dissolved in 1 mL serum free medium, and was added to each well, and were incubated for 4 h. Then the solution was removed and was replaced with 200 μL DMSO (dimethylsulfoxide). After shaking the plates for 15 min, the absorbance was measured at 570 nm, and the reference wavelength of 690 nm on an ELISA microplate reader (Bio-Tek Instruments).

To assess the cytotoxicity of HHC36 on CaP, three groups of samples, Ti, CaP, and CaP-AMP, were investigated in triplicate by the same MTT assay procedure. 10^4 of cell dispersion were seeded on each sample and the cells were allowed to attach to each sample for 2 h before adding the culture medium. Fresh medium was replaced every 2 days and MTT assay was carried out after 1, 2, and 5 days.

Cell attachment and morphology

The morphology and adherence of cells were investigated by culturing the MG-63 cells on specimens. By incubating the confluent cells with 0.25% trypsin-0.1% ethylenediaminetetraacetic acid (trypsin/EDTA) solution for 5 min, adequate number of cells was detached from culture flask, and centrifuged at 400*g* for 10 min to be used for each experiment.

For cell adhesion experiments, samples were first washed with 70% ethanol, and PBS, respectively, three times each. Then, MG-63 cells were seeded on Ti, CaP, and CaP-AMP six samples of each at a density of 5×10^5 cells per sample. After 4 h the specimens were rinsed with PBS to remove nonadherent cells and samples were digested with 0.5 mL of trypsin/EDTA for 10 min in incubator. Subsequently, a 0.5 mL culture medium was added to each sample to stop the trypsinization, and the cell quantity was counted by hematocytometer using a microscope. Cell attachment efficiency was presented by the percentage of number of attached cells divided by number of seeded cells.

To study the cell morphology and proliferation, specimens were sterilized and MG-63 cells were cultured identical as described. Then, 10^4 cells per sample was used after 4 h and 1-day incubation for fluorescence analysis. The specimens were washed with PBS, and fixed using 4% paraformaldehyde. The fixed cells were rinsed with PBS, and soaked into permeabilization buffer for 20 min at room temperature. Subsequently, the cytoskeletal filaments of cells were stained using rhodamine-phalloidin F-actin (Invitrogen), and DNA staining was performed by 4′,6-diamidino-2-phenylindole (Invitrogen). The samples were then

mounted on μ-slides (ibidi) and analyzed with confocal laser scanning microscopy (FV1000 Olympus).

Surgery and implantation procedure

For in vivo rabbit study, a total of 25 adult New Zealand white female rabbits weighting 3.5 to 5 kg were randomly distributed to three groups of implants, Ti (5 rabbits), CaP (10 rabbits), and CaP-AMP (10 rabbits). All rabbits were weighed at regular intervals but no attempt was made to standardize weights. The animals were fed with standard diet and observed on daily basis for signs of pain, infection, weight loss, and wound healing. Fifty cylindrical implants, etched Ti ($n = 10$), CaP ($n = 20$), and CaP-AMP ($n = 20$) were seal-packed and beta-ray sterilized (25 to 27 kGy; Iotron Technologies, Port Coquitlam, British Columbia, Canada). Surgery was performed under sterile conditions and general anesthesia. The animals were positioned supine with their legs shaved and decontaminated with a povidine and 70% alcohol. For implantation, an incision of 3 cm was made using a scalpel blade on the lateral aspect of the distal portion of the femur. The bone was exposed by splitting vastus lateralis. To avoid thermal damage to bone, a 4.37-mm hole was created perpendicular to the distal femoral condyle bilaterally using sequential low speed drilling of growing diameter (1.95, 3.18, and 4.37 mm) with saline irrigation. After verifying the depth of the hole with a gauge, the implants were press-fitted into the hole. The wound was closed in layers using standard techniques. Each rabbit received two identical implants, one on each femur. After six weeks all rabbits were euthanized with intravenous injection of Pentobarbital (2 mg/kg), and the femura were harvested. The implants' positions in the femurs were examined with a fluoroscope [Figure 1(a)]. The animal study protocol was approved by the Animal Care Committee of the University of British Columbia.

Histological processing and evaluation

The harvested femora were cleaned and the implants and the surrounding tissues were fixed and stored in 10% formalin solution before histological processing. All specimens were then dehydrated in a graded series of ethanol washings (70–100%), infiltrated, and embedded in epoxy resin (Spurr; Canemco, Canton de Gore, Quebec, Canada) according to standard histological procedure.[32] After polymerization the samples were sectioned longitudinally in three parallel course slices, 200, 850, and 1500 μm deep from implant surface, with each slice roughly perpendicular to the long axis of the femur. Each section was ground, polished, and sputtered with gold-palladium alloy, and examined with backscattered electron microscope (BSE) at 20 kV, 25 times magnification, and 27 mm of working distance, (S3000N; Hitachi, Tokyo, Japan). To create the final image, three images taken from each sample were merged together.

Bone growth in the gap region and on the implant surface was quantified by analyzing the BSE images using image analysis software (Clemex Vision PE 3.5; Clemex Technologies, Longueuil, Quebec, Canada). Four distinct materials in each image (titanium, bone cement caps, new grown bone, and epoxy) were discriminated in grayscale spectrum. The analysis provided quantitative data on the total gap and, total area of bone-gap filling (new bone formation in the gap created by caps) and bone on-growth (new bone formation in direct contact on the implant surface).

Statistics

"Primer of Biostatistics" software was used to assess the difference between the testing groups using one-way ANOVA (analysis of variance). A significant difference was considered when p-value was 0.05 or less, indicating 95% confidence limit.

RESULTS

Cytotoxicity

The MTT absorbance values reporting on the cytotoxicity of different concentrations of HHC36 and Tet213 AMPs revealed that there was a significant difference between two peptides in terms of retention of cell metabolic activity. While HHC36 showed cytotoxicity at concentrations greater than 200 μg/mL ($p = 0.08$ at 200 μg/mL, and $p = 0.01$ at 300 μg/mL), Tet213 exhibited higher cytotoxicity with significant effects at concentrations greater than 50 μg/mL ($p = 0.06$ at 50 μg/mL, and $p < 0.01$ at 75 μg/mL) compared with the negative control [Figure 2(a)]. Therefore most subsequent experiments employed HHC36 as the coating AMP. F2

In another MTT assay carried out on CaP-HHC36 using Ti and CaP (with no AMP loaded) as negative controls, it was observed that the cytocompatibility of HHC36 loaded specimens did not show any significant difference compared with controls ($p > 0.05$) [Figure 2(b)]. On the basis of the measurement in the next section and assuming 100% release of peptide in this cytotoxicity assay, the concentration of AMP in 1 mL of cell suspension would be ~70 μg/mL.

AMP loading and release

The tryptophan absorbance peak at 280 nm in the UV/Vis spectra was used for AMP quantification. Tests on standard solutions showed excellent linear relationships between peak intensity and AMP concentration in the ranges of 2–100 μg/mL (R^2 =0.999). Based on this calibration, the amount of AMP loaded on CaP samples was 34.7 ± 4.2 μg/cm^2.

Figure 3 shows the amount of AMP eluted from CaP-coated Ti samples over a 7-day period. The results indicate that 71.2% of AMP was eluted in the first 30 min; the number reached 84.3% in 150 min and 90.8% after 1-day release. This high release rate at the early time points was followed by a slow and steady release for days (Figure 3). After 7 days of this experiment, intact coatings were still observed on the Ti surfaces. F3 AQ2

Antimicrobial activity

The antimicrobial activities of CaP-AMP against *S. aureus* and *P. aeruginosa* are shown in Figure 4. The negative controls in the assay contained the same quantity of bacteria F4

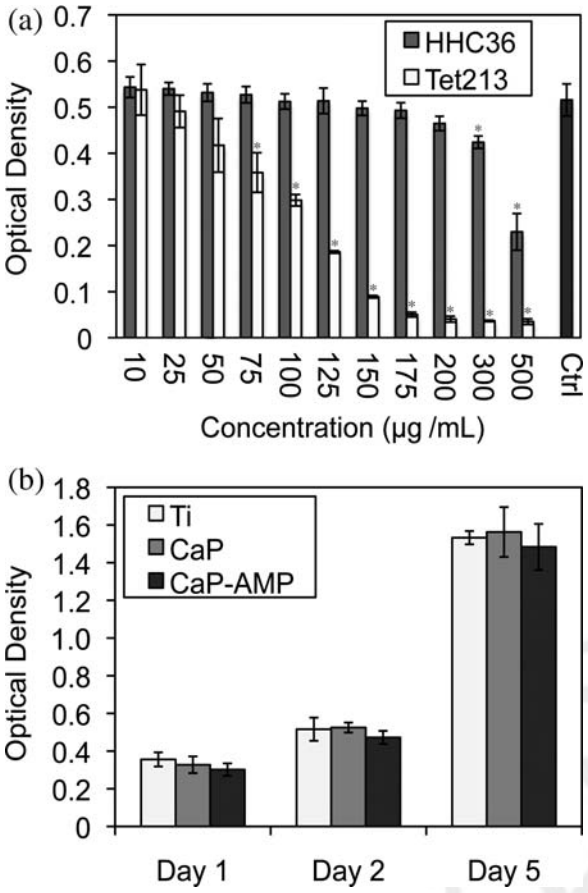

FIGURE 2. (a) The MTT assay of MG-63 cells cultured with various concentrations of HHC36 and Tet213 alone. Significant differences were observed in the cytotoxicity of the two AMPs. While HHC36 showed cytotoxicity at concentrations of 300 μg/mL and above ($p = 0.01$ at 300 μg/mL), the Tet213 exhibited cytotoxicity at relatively lower concentrations μg/mL ($p < 0.01$ at 75 μg/mL) compared with the negative control. (b) No increased cytotoxicity was observed on CaP-AMP samples compared to controls ($p > 0.05$). The higher level at day 5 was due to increased growth of cells after 5 days.

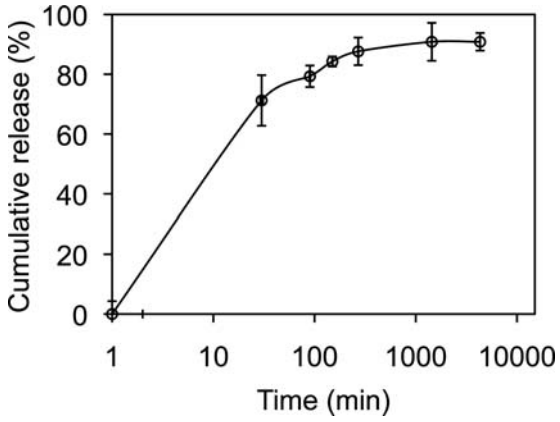

FIGURE 3. The cumulative *in vitro* release of HHC36 from CaP coating in PBS after 30 min, 90 min, 150 min, 270 min, 1 day, 3 day, and 7 day ($n = 3$). Error bars represent the means ± standard deviation. Quantification of total AMP concentration loaded on CaP showed (34.7 ± 4.2 μg/cm^2) using UV/Vis spectroscopy at 280 nm based on the use of external standards ($n = 6$)

incubated in fresh MHB under the same condition without AMPs. The results illustrated that CaP-AMP was able to kill 100% bacteria of both strains in less than 150 min, while bacteria colonies in controls grew by more than a hundred fold. If we assume 100% release of peptide in the antimicrobial assay, the maximum concentration of AMP in 400 μL of bacterial suspension would be ~174 μg/mL.

MG-63 osteoblast-like cell attachment and morphology

The number of attached MG-63 cells on Ti, CaP, and CaP-AMP were measured after 4 h of culturing (Figure 5). The efficiency of adhered cells on Ti, CaP, and CaP-AMP were calculated to be 55.8, 73.3, and 77.6%, respectively, indicating a significant increase ($p < 0.01$) of cell attachment on CaP and CaP-AMP.

The morphology of MG-63 cells was evaluated by confocal laser scanning microscopy. During the first 4 h, active cells spread on all substrates [Figure 6(a–c)]. After 1 day, cells spread and extensively covered the surface of the CaP and CaP-AMP samples, while fewer cells were observed on Ti samples [Figure 6(d–f)]. The stretching of cells on the CaP-AMP samples indicated these cells were interacting with each other [Figure 6(e,f)].

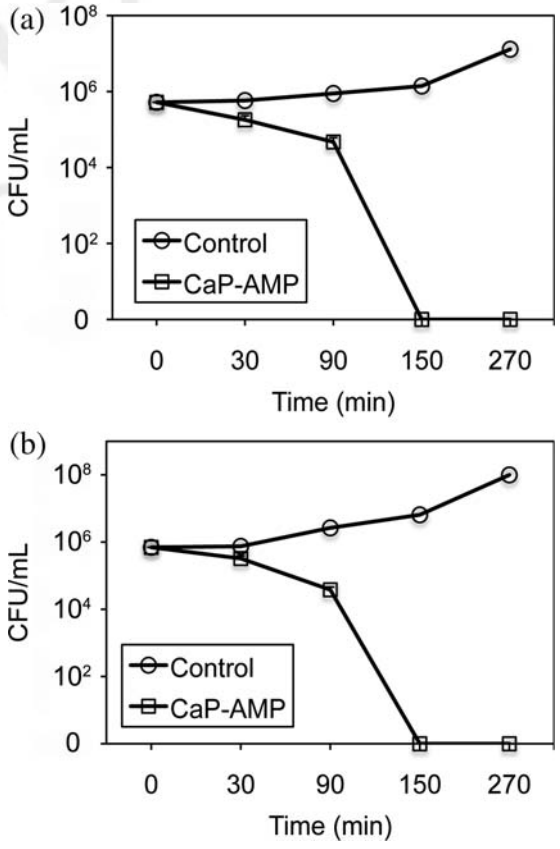

FIGURE 4. Antimicrobial activity of the CaP-AMP (HHC36) samples against (a) *S. aureus*, (b) *P. aeruginosa*. The specimens CaP-AMP were able to entirely kill both strains in less than 150 min.

ID: ananda | Black Lining: [ON] | Time: 17:00 | Path: N:/3b2/JBMB/Vol00000/120044/APPFile/JW-JBMB120044

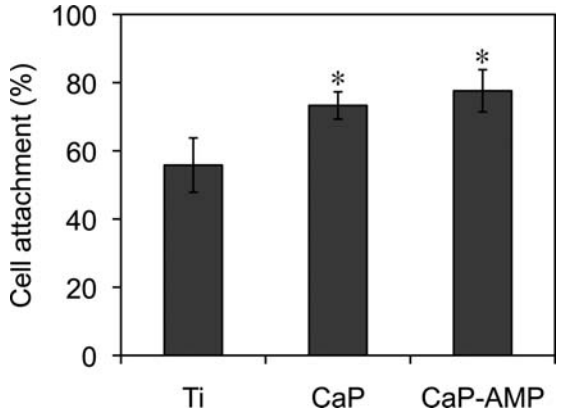

FIGURE 5. Cell attachment efficiency of specimens after seeding 5×10^5 MG-63/sample after 4 h. The efficiency of adhered cells on Ti, CaP, and CaP-AMP (HHC-36) were calculated to be 55.8, 73.3, and 77.6%, respectively. Asterisk indicates significant difference between cell attachment efficiency on Ti and other groups ($p < 0.01$).

Bone growth analysis

After surgery, one rabbit from each group was excluded from the histological study due to either improper implantation or weight loss exceeding 20%. The remaining rabbits had no signs of severe reaction, infection or other abnormalities. Backscattered electron microscopy confirmed that newly formed bone had grown into the gap region in all three groups of implants (Figure 7). The bone growth results are summarized in Table I and Figure 8. The average bone growth slightly increased from Ti, CaP-coated Ti (CaP), to AMP-loaded CaP (CaP-AMP), but no significant differences ($p > 0.05$) were observed among the groups. However, the contact length between bone and the implant showed a significant difference ($p = 0.01$) between the uncoated Ti and the other two coated surfaces, indicating considerable bone on-growth on CaP (~54%) and, CaP-AMP (~60%) compared with Ti (~ 36%) surfaces. Compared with the CaP group, the group treated with the AMP had a slight increase in the percentage of bone contact length (by ~6%). However this increase was not significant ($p = 0.13$) (Figure 8).

DISCUSSION

One concern regarding the local delivery of antibiotics in orthopedics is the relative inhibition of osseointegration.[33] High doses of antibiotics often impair cell viability and osteogenic activity.[13] Therefore, the development and selection of antimicrobial agents for local delivery onto orthopedic implants should consider osteoconductivity. Results from the current study demonstrate that locally delivering antimicrobial peptides using calcium phosphate coatings can effectively kill bacteria *in vitro*, but does not impair bone growth. In fact, local delivery of HHC36 led to a moderate enhancement in bone growth, although the increase was not significant. In our study, the *in vivo* test has been used to investigate the bone growth in the presence of AMP coating and does not involve infection study.

Extensive effort has been made to identify the AMPs' antimicrobial mechanisms of surface associated AMPs.[34–48] Recent studies indicated that the killing mechanism of AMPs is based on the high density of polycationic charges in vicinity of the surface, which would initiate an

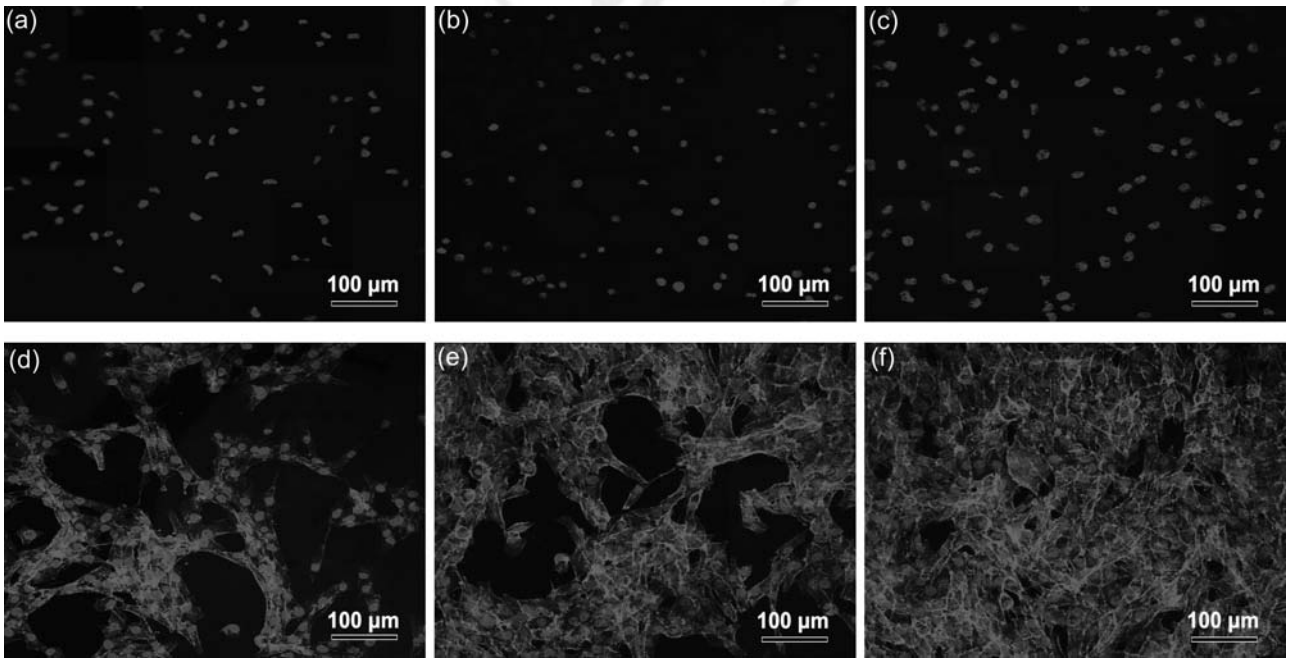

FIGURE 6. (a) Confocal laser scanning of cells cultured on (a) Ti, (b) CaP-Tet213, and (c) CaP-HHC36 after 4 h, showing the distribution and adherence of MG-63 cells. Confocal laser scanning of cells cultured on (d) Ti, (e) CaP-Tet213, and (f) CaP-HHC36 after 1 day, well-defined presence of stress fibers implies the firm attachment of cells, sheet-like proliferation of cells, and distribution of focal contacts on the coating and between cells on CaP-AMP coating. Blue and red colors represent DNA and F-actin staining. [Color figure can be viewed in the online issue, which is available at wileyonlinelibrary.com.]

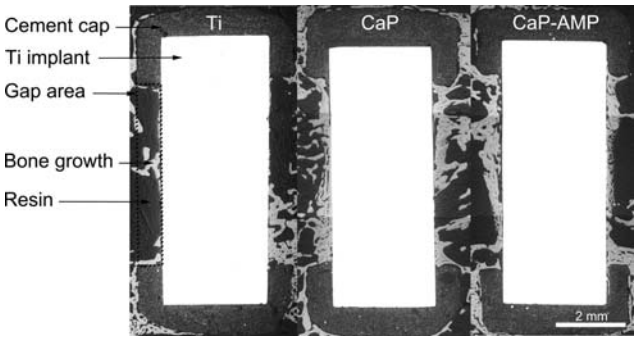

FIGURE 7. Representative BSE images of the implant surfaces of each group displaying bone growth expanding into gap. Dotted line shows the bone growth region and magnified images exhibit random bone on-growth on each interface.

electrostatic interaction with polyanionic outer layer of microbes. The high local concentration of AMPs would then displace positively charged ions, leading to membrane disruption.[19,39] The ability of AMPs to selectively interact with the bacterial cells rather than the mammalian cells makes them highly antimicrobial with low toxicity for host cells. The major factor that contributes to the selectivity property of AMPs is the cationic property. The surface of the bacterial membranes is more negatively charged than mammalian cells. This will lead to higher affinity of AMPs for bacterial surfaces. Moreover, mammalian cell membranes contain high amounts of cholesterol, which is absent in bacteria cells, as membrane stabilizing agents and inhibitor of AMP activites.[40,41] Nevertheless, different AMPs vary in their cytotoxicity towards host cells.[40,41] For the two potent antimicrobial peptides compared in this study, HHC36 and Tet213, despite their shared peptide sequence, the addition of one cysteine in Tet213 substantially lowered the minimal osteoblast toxicity concentrations from 300 to 75 μg/mL [Figure 2(a)].

In this work, the substantial amount of HHC36 (34.7± 4.2 μg/cm^2) loaded on CaP coating can be attributed to the affinity between the positively charged side groups of HHC36 and negatively charged phosphate groups in the CaP and the porous structure of the coating. HHC36 with the sequence of KRWWKWWRR-NH_2 has a cationic charge of +5, and a theoretical isoelectric point of 12.31. Such a high IE point makes HHC36 highly positive at working pH (7.4), and provides numerous opportunities for positively charged Arg and Lys residues to interact with CaP. According to Amina et al., the presence of two adjacent basic residues (Arg-Arg, in our case) might create a "covalent-like" stability with phosphate under the right electrostatic conditions.[34] This explanation however is not entirely compatible with the rapid initial release kinetics of the peptide from CaP surfaces although it may help to explain the subsequent slow release.

An ideal implant related infection treating method would locally release high concentration of antibiotic initially followed by an effective long-term release, while maintaining osseointegration at the same time.[35] In this study, following the initial burst stage, the coating released 71% of AMP in the first 30 min and 90% within 24 h (Figure 3). HHC36 has a very low minimum inhibitory concentration (MIC) of 1.4 to 2.9 μ*M* against *S. aureus* (MDR) and 0.7 to 5.7 μ*M* against *P. aeruginosa* (MDR), with the half maximal inhibitory concentration (IC_{50}) value of 0.13.[28,29] The total AMP loaded on to each implant is calculated to be ~28 μg. If we assume the entire AMP is released to the trabecular bone region that is 5–100 times of the gap volume, the concentration of AMP would be 106.6–5.3 μ*M*. Therefore, the local AMP release, even though relatively quick, should enable elimination of a significant number of bacteria introduced to the surgical site in the first day. Since current animal study did not involve an infection model, the *in vivo* efficacy of the AMP loaded implants is to be confirmed.

To date there have been few reports on *in vivo* bone growth onto antimicrobial peptide loaded orthopedic implants. Most of studies on implant associated antimicrobial agents have focused on conventional antibiotic delivery systems especially through bone cement.[36–38] A relevant report investigated the *in vivo* release of the antimicrobial peptide hLF1-11 from calcium phosphate cement.[42] Despite the initial burst release of this AMP, it was concluded that hLF1-11 could be considered as a prophylactic agent for osteomyelitis treatment. No inflammation or necrosis signs were observed in bone grown into the cement.[42,43] In our study, the backscattered electron microscopy study of the new bone grown on the CaP-AMP implants showed normal bone structure with no distinguishable differences between CaP-AMP and CaP controls. Assuming 100% release of the AMP into the gap region only (35.3 mm^{3}of volume), the

TABLE I. Histomorphometric Bone (a) Gap Filling, and (b) Bone On-Growth Data Are Expressed as Mean ± Standard Deviation

Implant	Bone Gap Filling (%)	Section 1	Section 2	Section 3
(a)				
Ti ($n = 8$)	28.5 ± 10.0	28.7 ± 11.8	29.1 ± 10.1	27.7 ± 11.0
CaP ($n = 18$)	30.1 ± 9.7	28.1 ± 8.5	30.8 ± 10.1	31.3 ± 11.0
CaP-HHC36 ($n = 18$)	32.8 ± 9.9	33.3 ± 11.6	32.6 ± 9.2	32.3 ± 10.1
(b)				
Ti ($n = 8$)	35.9 ± 10.4	32.5 ± 14.9	32.7 ± 8.8	42.6 ± 8.8
CaP ($n = 18$)	53.7 ± 12.2	54.5 ± 12.9	51.0 ± 13.2	55.5 ± 13.0
CaP-HHC36 ($n = 18$)	60.4 ± 11.9	60.7 ± 14.7	56.6 ± 14.6	63.8 ± 9.4

Sections 1, 2 and 3 were in three parallel course slices, with 200, 850 and 1500 μm deep from the tangent surface of implants, respectively.

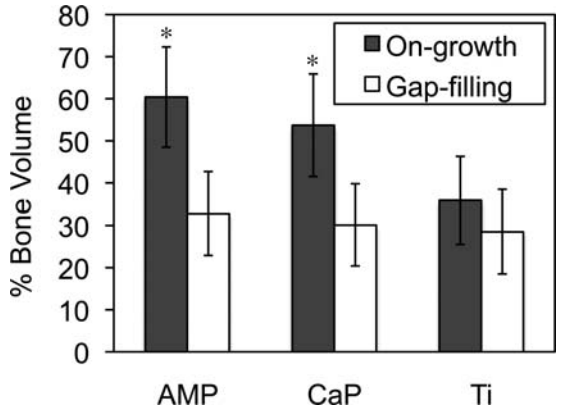

FIGURE 8. Total gap filling and bone on-growth (mean values and standard deviations) of three sections. No significant statistical difference was observed in terms of gap-filling between three groups. Bone on-growth values however revealed different results. Asterisk indicates a significant difference ($p = 0.01$) between Ti and other groups, indicating considerable contact bone growth on CaP and, CaP-AMP (HHC36) versus Ti samples. Compared with the CaP group, the group treated with the AMP had a relative increase in the percentage of the length of the implant that was in contact with new bone. However this increase was not significant ($p = 0.13$).

local peptide concentration would be 793 μg/mL, which is higher than the cytotoxicity concentration (200 μg/mL). Nevertheless, *in vivo* bone growth study demonstrated the calculated high AMP concentration does not lead to impaired osteoconductivity. One possible explanation is the dynamic fluid flow in and out of the gap region. The observed slightly higher total new bone formation on CaP-AMP than CaP implants in Table I may imply a potential role of AMP (HHC36) in stimulating bone growth *in vivo*. In this regard synthetic cationic peptides including many AMPs have the ability to modulate innate immunity in host cells including stimulation of wound healing, and neutralization of some characteristics of inflammation such as endotoxemia.[44,45]

It is well understood that OCP plate-like coating improves osteoblast adhesion, spreading and proliferation by enhancing the focal contacts or selectively adsorption of proteins.[46,47] Our *in vitro* cell attachment and proliferation test showed that the integration of HHC36 into the OCP coating did not inhibit the cell attachment and proliferation. The extensive bone on-growth on CaP-AMP and CaP surfaces in the animal experiment also confirmed a positive bone response to the combination of AMP and CaP coating (Figure 7). This is consistent with the observation that the AMP concentration on the CaP coating (~70 μg per sample/1 mL culture media), was lower than the minimal cytotoxic concentration of HHC36 (<200 μg/mL) [Figure 2(a)]. The observation of adhering MG-63 cells by fluorescent microscopy after 4 h of incubation [Figure 6(a–c)], showed that cells attached, and strongly bonded to the substrate on coating. The even distribution of stress fibers after 1 day implied firm attachment and might be an evidence for lower motility of cells [Figure 6(e,f)]. It could be seen in Figure 6(e,f) that in contrast to uncoated Ti surface, the cells in mitosis state reached confluency covering almost all the surface on both samples treated with AMP, indicating cell proliferation.

CONCLUSIONS

This study shows that osteoconductive OCP coating loaded with HHC36 AMP has the potential to serve as an antimicrobial coating while maintaining osseointegration. *In vitro* tests concluded that this AMP-CaP coating can effectively kill *S. aureus*, and *P. aeruginosa* bacteria without negatively affecting MG-63 osteoblast like cells. Loading of AMP HHC36 did not impair *in vivo* bone growth onto the implants. There was *a s*ignificant bone on-growth on CaP-AMP as compared with the negative control. The ELD calcium phosphate coating, and the simplicity of AMP loading provide substantial advantages for this antimicrobial coating.

ACKNOWLEDGMENTS

R.W. is incumbent of the Canada Research Chair in Biomaterials while REWH holds a Canada Research Chair in Health and Genomics. The authors wish to thank Mr. Reza Falsafi, Ms. Jelena Pistolic and Ms. Shaan Gellatly for kindly assisting in cell and bacteria culture, Ms. Stephanie Smith for assisting in surgery, and Dr. Danmei Liu for providing histology protocols. They are also grateful for the discussions with Dr. Jayachandran N Kizhakkedathu, Dr. Jason Kindrachuk, Dr. Ben Chew, and Dr. Donald Brooks.

REFERENCES

1. Trampuz A, Zimmerli W. Antimicrobial agents in orthopaedic surgery—Prophylaxis and treatment. Drugs 2006;66:1089–1105.
2. Trampuz A, Widmer AF. Infections associated with orthopedic implants. Curr Opin Infect Dis 2006;19:349–356.
3. Costerton JW, Montanaro L, Arciola CR. Biofilm in implant infections: Its production and regulation. Int J Artif Organs 2005;28: 1062–1068.
4. Costerton JW, Stewart PS, Greenberg EP. Bacterial biofilms: A common cause of persistent infections. Science 1999;284:1318–1322.
5. Donlan RM, Costerton JW. Biofilms: Survival mechanisms of clinically relevant microorganisms. Clin Microbiol Rev 2002;15:167–193.
6. Rogers SS, van der Walle C, Waigh TA. Microrheology of bacterial biofilms in vitro: *Staphylococcus aureus* and *Pseudomonas aeruginosa*. Langmuir 2008;24:13549–13555.
7. Lyczak JB, Cannon CL, Pier GB. Establishment of *Pseudomonas aeruginosa* infection: Lessons from a versatile opportunist. Microbes Infect 2000;2:1051–1060.
8. Rao NL, Ziran BH, Lipsky BA. Treating osteomyelitis: Antibiotics and surgery. Plast Reconstr Surg 2011;127:177S–187S.
9. Zimmerli W, Trampuz A, Ochsner PE. Prosthetic-joint infections. N Engl J Med 2004;351:1645–1654.
10. Kazemzadeh-Narbat M, Kindrachuk J, Duan K, Jenssen H, Hancock REW, Wang R. Antimicrobial peptides on calcium phosphate-coated titanium for the prevention of implant-associated infections. Biomaterials 2010;31:9519–9526.
11. Lauderdale KJ, Malone CL, Boles BR, Morcuende J, Horswill AR. Biofilm dispersal of community-associated methicillin-resistant Staphylococcus aureus on orthopedic implant material. J Orthop Res 2010;28:55–61.
12. Darouiche RO. Treatment of infections associated with surgical implants. N Engl J Med 2004;350:1422–1429.
13. Rathbone CR, Cross JD, Brown KV, Murray CK, Wenke JC. Effect of various concentrations of antibiotics on osteogenic cell viability and activity. J Orthop Res 2011;29:1070–1074.
14. Zhao L, Chu PK, Zhang Y, Wu Z. Antibacterial coatings on titanium implants. J Biomed Mater Res B Appl Biomater 2009;91:470–480.

15. Francolini I, Donelli G. Prevention and control of biofilm-based medical-device-related infections. FEMS Immunol Med Microbiol 2010;59:227–238.
16. Rotem S, Mor A. Antimicrobial peptide mimics for improved therapeutic properties. Biochim Biophys Acta 2009;1788:1582–1592.
17. Yeaman MR, Yount NY. Mechanisms of antimicrobial peptide action and resistance. Pharmacol Rev 2003;55:27–55.
18. Hancock REW, Lehrer R. Cationic peptides: A new source of antibiotics. Trends Biotechnol 1998;16:82–88.
19. Hilpert K, Volkmer-Engert R, Walter T, Hancock REW. High-throughput generation of small antibacterial peptides with improved activity. Nat Biotech 2005;23:1008–1012.
20. Jenssen H, Hamill P, Hancock REW. Peptide antimicrobial agents. Clin Microbiol Rev 2006;19:491–511.
21. Brogden KA. Antimicrobial peptides: Pore formers or metabolic inhibitors in bacteria? Nat Rev Microbiol 2005;3:238–250.
22. Gidalevitz D, Ishitsuka Y, Muresan AS, Konovalov O, Waring AJ, Lehrer RI, et al. Interaction of antimicrobial peptide protegrin with biomembranes. Proc Natl Acad Sci USA 2003;100:6302–6307.
23. Madera L, Ma S, Hancock REW. Host defense (antimicrobial) peptides and proteins. Immune Response Infect 2011:57–67.
AQ3
24. Liu S, Yang H, Wan L, Cai H-W, Li S-F, Li Y-P, et al. Enhancement of cytotoxicity of antimicrobial peptide magainin II in tumor cells by bombesin-targeted delivery. Acta Pharmacol Sin 2011;32:79–88.
25. Gao G, Lange D, Hilpert K, Kindrachuk J, Zou Y, Cheng JTJ, et al. The biocompatibility and biofilm resistance of implant coatings based on hydrophilic polymer brushes conjugated with antimicrobial peptides. Biomaterials 2011;32:3899–3909.
26. Fan YW, Duan K, Wang RZ. A composite coating by electrolysis-induced collagen self-assembly and calcium phosphate mineralization. Biomaterials 2005;26:1623–1632.
27. Garbuz DS, Hu Y, Kim WY, Duan K, Masri BA, Oxland TR, et al. Enhanced gap filling and osteoconduction associated with alendronate-calcium phosphate-coated porous tantalum. J Bone Joint Surg Am 2008;90:1090–1100.
28. Fjell CD, Jenssen H, Hilpert K, Cheung WA, Pante N, Hancock REW, et al. Identification of novel antibacterial peptides by chemoinformatics and machine learning. J Med Chem 2009;52:2006–2015.
29. Cherkasov A, Hilpert K, Jenssen Hv, Fjell CD, Waldbrook M, Mullaly SC, et al. Use of artificial intelligence in the design of small peptide antibiotics effective against a broad spectrum of highly antibiotic-resistant superbugs. ACS Chem Biol 2008;4:65–74.
30. Pace CN, Vajdos F, Fee L, Grimsley G, Gray T. Howtomeasure and predict the molar absorption-coefficient of a pretein. Protein Sci 1995;4:2411–2423.
31. Delhaye S, Landry J. High-performance liquid chromatography and ultraviolet spectrophotometry for quantitation of tryptophan in barytic hydrolysates. Anal Biochem 1986;159:175–178.
32. Thomas W. Bauer DM. Handbook of Histology Methods for Bone and Cartilage. Totowa, New Jersey: Humana Press; 2003.
33. Brown K, Li B, Guda T, Guelcher S, Wenke J. Local antibiotics do not inhibit bone growth when administered with growth factro. J Bone Joint Surg Br B 2011;93:100.
34. Woods AS, Ferre S. Amazing stability of the arginine-phosphate plectrostatic interaction. J Proteome Res 2005;4:1397–1402.
35. Wu P, Grainger DW. Drug/device combinations for local drug therapies and infection prophylaxis. Biomaterials 2006;27: 2450–2467.
36. Gerhart TN, Roux RD, Horowitz G, Miller RL, Hanff P, Hayes WC. Antibiotic release from an experimental biodegradable bone-cement. J Orthop Res 1988;6:585–592.
37. Joosten U, Joist A, Gosheger G, Liljenqvist U, Brandt B, von Eiff C. Effectiveness of hydroxyapatite-vancomycin bone cement in the treatment of *Staphylococcus aureus* induced chronic osteomyelitis. Biomaterials 2005;26:5251–5258.
38. Schnieders J, Gbureck U, Thull R, Kissel T. Controlled release of gentamicin from calcium phosphate—poly(lactic acid-co-glycolic acid) composite bone cement. Biomaterials 2006;27: 4239–4249.
39. Hilpert K, Elliott M, Jenssen H, Kindrachuk J, Fjell CD, Korner J, et al. Screening and characterization of surface-tethered cationic peptides for antimicrobial activity. Chem Biol 2009;16:58–69.
40. Glukhov E, Stark M, Burrows LL, Deber CM. Basis for selectivity of cationic antimicrobial peptides for bacterial versus mammalian membranes. J Biol Chem 2005;280:33960–33967.
41. Mello Charlene M, Soares Jason W. Membrane selectivity of antimicrobial peptides. Microbial Surfaces ACS 2008:52–62.
42. Stallmann HP, de Roo R, Faber C, Amerongen AVN, Wuisman P. In vivo release of the antimicrobial peptide hLF1–11 from calcium phosphate cement. J Orthop Res 2008;26:531–528.
43. Faber C, Stallmann HP, Lyaruu DM, Joosten U, von Eiff C, Amerongen AV, et al. Comparable efficacies of the antimicrobial peptide human lactoferrin 1–11 and gentamicin in a chronic methicillin-resistant *Staphylococcus aureus* osteomyelitis model. Antimicrob Agents Chemother 2005;49:2438–2444.
44. Hancock REW. Cationic peptides: Effectors in innate immunity and novel antimicrobials. Lancet Infect Dis 2001;1:156–164.
45. Gough M, Hancock R, Kelly N. Antiendotoxin activity of cationic peptide antimicrobial agents. Infect Immun 1996;64:4922–4927.
46. Chang YL, Stanford CM, Wefel JS, Keller JC. Osteoblastic cell attachment to hydroxyapatite-coated implant surfaces in vitro. Int J Oral Maxillofac Implants 1999;14:239–247.
47. Deligianni DD, Katsala ND, Koutsoukos PG, Missirlis YF. Effect of surface roughness of hydroxyapatite on human bone marrow cell adhesion, proliferation, differentiation and detachment strength. Biomaterials 2001;22:87–96.